

# Surface and Catalytic Chemistry of Small Hydrocarbons on Oxidized Molybdenum

Gefei Wu, Brian Bartlett, and Wilfred T. Tysoe\*

Department of Chemistry and Laboratory for Surface Studies, University of Wisconsin–Milwaukee, Milwaukee, Wisconsin, 53211-3029

Received July 3, 1997. In Final Form: November 25, 1997

It is shown that model oxides grown on metallic substrates catalyze propylene metathesis to form ethylene and butene with an activity that mimics that of supported catalysts for reaction below ~650 K. Another reaction regime is found for olefin metathesis above ~650 K, where the reaction proceeds with a much higher activation energy of ~60 kcal/mol. Unfortunately, alkenes do not react to any detectable extent on the model oxide surfaces in ultrahigh vacuum. However, the high-temperature (> 650 K) metathesis rate is found to be affected by the presence of oxygen overlayers, which also modify the chemistry of alkenes on Mo(100) in ultrahigh vacuum. It is found that methane is formed by reaction of alkenes on O/Mo(100). The only other products detected are ascribed to either hydrogenation or total thermal decomposition into carbon and hydrogen. It is shown, using iodine-containing molecules to graft hydrocarbon fragments onto the surface, that alkenes can dissociate, forming carbenes which react to yield methane. This chemistry is in accord with that found catalytically at high temperatures, where the product distribution from the reaction of ethylene is well described by a Schulz–Florey distribution and the product distribution from propylene is well described by copolymerization of carbenes and methyl carbenes.

## Introduction

The randomization of alkylene groups in alkenes, that is, their metathesis, is essentially thermoneutral, since the number and type of carbon–carbon bonds are conserved for reactants and products. The reaction was discovered in 1931,<sup>1</sup> where it was shown by Schneider and Frölich that heating propylene to high temperatures indeed formed the thermodynamically predicted products. The rate is limited by the high activation energy for the reaction and is a classical example of a Woodward–Hoffmann (electronic-symmetry)-forbidden reaction.<sup>2</sup> A heterogeneous catalyst for the reaction was discovered over 30 years later by Banks and Bailey,<sup>3</sup> who found that alumina-supported molybdena catalyzed the metathesis of propylene to ethylene and butene with rather high selectivity below ~650 K with an activation energy of ~6 kcal/mol,<sup>4,5</sup> substantially lower than the value in the absence of a catalyst. Early theories for the effectiveness of the metathesis catalyst were framed in terms of lowering the activation barrier of a surface C<sub>4</sub> intermediate transition state<sup>6–8</sup> by having the substrate orbital participate in bonding with the reaction transition state and act as an electron sink to lower the transition state energy. This situation has been discussed in detail in a classical paper by Schachtschneider.<sup>9</sup> However, work with *homogeneous* catalysts resulted in the proposal of an alternative, two-step model which suggested that reaction was initi-

ated by the formation of a surface carbene which, in the homogeneous phase, was often included in the catalyst itself or provided by reaction with a cocatalyst. The carbene is then proposed to provide the active site for reaction by reacting with an alkene to produce a metalacyclic intermediate.<sup>10–26</sup> This can potentially react via several routes; for example, reductive elimination yields cyclopropane<sup>27</sup> or a hydrogen transfer produces an alkene.<sup>28</sup> Both of these reactions, of course, destroy the initial carbene active site. Finally, the metallacycle can react via the reverse of its formation pathway to re-form an alkene and a surface carbene, resulting in an overall metathesis reaction, since a carbon–carbon double bond has effectively been broken and re-formed.<sup>10–26</sup> In fact, in this pathway, complete scission of the double bond is not required, presumably resulting in a lowering of the reaction activation energy. The carbene can also be consumed by reacting with other carbenes analogously to

\* To whom correspondence should be addressed. Telephone: (414) 229-5222. Fax: (414) 229-5036. E-mail: wtt@csd.uwm.edu.

(1) Schneider, V.; Frölich, P. K. *Ind. Eng. Chem.* **1931**, *23*, 1045.  
 (2) Woodward, R. B.; Hoffmann, R. *The Conservation of Orbital Symmetry*; Academic Press Inc.: New York, 1972.  
 (3) Banks, R. L.; Bailey, G. C. *Ind. Eng. Chem. Prod. Res. Dev.* **1965**, *94*, 60.  
 (4) Ogata, E.; Kamiya, Y. *Chem. Lett.* **1973**, 603.  
 (5) Bradshaw, C. P. C.; Howman, E. J.; Turner, L. *J. Catal.* **1967**, *7*, 269.  
 (6) Adams, C. T.; Brandenberger, S. G. *J. Catal.* **1969**, *13*, 360.  
 (7) Crain, D. L. *J. Catal.* **1969**, *13*, 110.  
 (8) Mol, J. C.; Mouljin, J. A.; Boelhouwer, C. *J. Catal.* **1968**, *11*, 87.  
 (9) Mango, F. D.; Schachtschneider, J. H. *J. Am. Chem. Soc.* **1969**, *91*, 1030.

(10) Hérisson, J. L.; Chauvin, Y. *Makromol. Chem.* **1970**, *141*, 161.  
 (11) Soufflet, J. P.; Commerce, D.; Chauvin, Y. C. R. *Hebd. Séances Acad. Sci., Ser. C.* **1973**, *276*, 169.  
 (12) Haines, R. J.; Leigh, G. *J. Chem. Soc. Rev.* **1975**, *4*, 155.  
 (13) Casey, C. P.; Burkhardt, T. J. *J. Am. Chem. Soc.* **1974**, *96*, 7808.  
 (14) Fischer, E. O.; Dotz, K. H. *Chem. Ber.* **1972**, *105*, 3966.  
 (15) Schrock, R. R. *J. Am. Chem. Soc.* **1974**, *96*, 6976.  
 (16) Schrock, R. R. *J. Am. Chem. Soc.* **1976**, *98*, 5399.  
 (17) Dolgoplosk, B. A. *Dokl. Chem.* **1974**, *216*, 380.  
 (18) Grubbs, R. H.; Burk, P. L.; Carr, D. D. *J. Am. Chem. Soc.* **1975**, *97*, 3265.  
 (19) Grubbs, R. H.; Carr, D. D.; Hoppin, C.; Burk, P. C. *J. Am. Chem. Soc.* **1976**, *98*, 3478.  
 (20) Katz, T. J.; Rothschild, J. *J. Am. Chem. Soc.* **1976**, *98*, 2519.  
 (21) Katz, T. J.; Hersch, W. H. *Tetrahedron Lett.* **1977**, 585.  
 (22) Casey, C. P.; Tuinstra, H. E.; Seaman, M. C. *J. Am. Chem. Soc.* **1976**, *98*, 608.  
 (23) Tebbe, F. N.; Parshall, G. W.; Ovenall, D. W. *J. Am. Chem. Soc.* **1979**, *101*, 5074.  
 (24) Wengorius, J.; Schrock, R. R.; Churchill, M. R.; Mussert, J. R.; Young, W. J. *J. Am. Chem. Soc.* **1980**, *102*, 4515.  
 (25) Howard, T. R.; Lee, J. B.; Grubbs, R. H. *J. Am. Chem. Soc.* **1980**, *102*, 6878.  
 (26) Grubbs, R. H.; Brunck, T. K. *J. Am. Chem. Soc.* **1972**, *94*, 25.  
 (27) McQuillan, F. J.; Powell, K. G. *J. Chem. Soc., Dalton Trans.* **1972** 2123.  
 (28) Millman, W. S.; Crespin, M.; Cirrillo, A. L.; Abdo, S.; Hall, W. K. *J. Catal.* **1979**, *60*, 404.

the polymerization step in the Fischer–Tropsch synthesis.<sup>29</sup> This is, of course, also effectively an olefin metathesis, since carbon–carbon bonds are cleaved and reassembled.

It is also found that the activity of the molybdenum (and also tungsten and rhenium) catalysts depends on the oxidation state of the metal<sup>30,31</sup> so that supported metallic (zero oxidation state) catalysts are considered to be completely inactive and that some higher oxidation state, often thought to be +4, is the most active for the reaction. The nature of the most active catalyst and possible pathways for the reaction are probed using surface science strategies on model catalyst samples in the following.

### Experimental Section

The experiments were performed on a range of pieces of apparatus, all of which have been discussed in detail elsewhere.<sup>32,33</sup> Temperature-programmed desorption data were collected on a bakeable, stainless steel chamber operating at a base pressure of  $\sim 5 \times 10^{-11}$  Torr which was equipped with capabilities for multistage, temperature-programmed desorption, low-energy electron diffraction and Auger spectroscopy. The sample could be heated to  $\sim 2100$  K using electron-beam heating and cooled to  $\sim 80$  K by thermal contact with a liquid-nitrogen-filled reservoir. Catalytic reactions were carried out in a chamber pumped by means of a diffusion pump and operated at a base pressure of  $1 \times 10^{-10}$  Torr.<sup>34</sup> This chamber also incorporated a coaxial, high-pressure reactor which could be pressurized to  $\sim 800$  Torr while maintaining ultrahigh vacuum in the rest of the apparatus. The gas was recirculated within the cell by means of a gas pump, and the reaction rate was determined by measuring the gas composition periodically by diverting a small portion of the reactant mixture to a gas chromatograph for analysis. Reaction rates are calculated directly from a product accumulation curve for low (<1%) conversions. This sample could also be heated to  $\sim 2000$  K and cooled by contact with a liquid-nitrogen-chilled reservoir.

Ultraviolet photoelectron spectra were obtained at the Wisconsin Synchrotron Radiation Center using the Aladdin storage ring.<sup>35</sup> The stainless steel, ultrahigh vacuum chamber used for these experiments operated at a base pressure of  $\sim 1 \times 10^{-10}$  Torr following bakeout and was attached to the end of a Mark V Grasshopper monochromator. The chamber was equipped with a quadrupole mass analyzer for residual gas analysis and to test gas purities. It was also equipped with a double-pass cylindrical mirror analyzer which was used to collect both Auger and photoelectron spectra.

The sample was cleaned by heating in  $\sim 2.5 \times 10^{-7}$  Torr of oxygen at 1200 K for 5 min to remove carbon and then rapidly heated in vacuo to 2100 K to remove oxygen. This resulted in the diffusion of further carbon to the surface, and this procedure was repeated until no impurities, particularly carbon, were noted on the surface after heating to 2100 K.

Oxygen overlayers were prepared by saturating the Mo(100) surface (20 L of O<sub>2</sub> exposure at 1050 K; 1 L =  $1 \times 10^{-6}$  Torr·s) and annealing to various temperatures to remove oxygen to obtain the requisite coverage. The adsorption of oxygen on Mo(100) has been studied very extensively,<sup>36–39</sup> and the oxygen coverages were reproduced from their characteristic LEED patterns and confirmed from their relative O/Mo Auger ratios (by monitoring the O KLL and Mo LMM Auger transitions). MoO<sub>2</sub> films were grown using a literature protocol,<sup>40</sup> which provides a surface

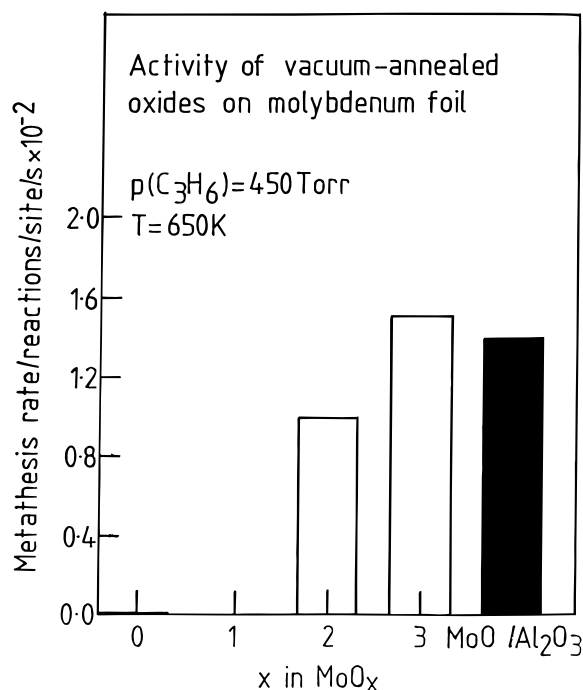


**Figure 1.** Relative activity of various model molybdenum oxides for olefin metathesis using 450 Torr of propylene for reaction at  $\sim 650$  K. Shown for comparison is the reactivity of a supported molybdenum oxide where the molybdenum loading is relatively high (18.6%<sup>42</sup>).

that is active for olefin metathesis, where metallic molybdenum was oxidized using  $3 \times 10^{-5}$  Torr of oxygen for 120 s with the sample heated to 1050 K.<sup>41</sup>

Alkenes were transferred to glass bottles, further purified by repeated bulb-to-bulb distillations, and stored in glass vessels until use. The oxygen (AGA Gas, Inc. 99%) was transferred from the cylinder to a glass bulb and also redistilled.

### Results

The metathesis activity, defined as the rate of ethylene and butene formation from the reaction of propylene, of various model molybdenum oxide catalysts was tested in the high-pressure reactor using 450 Torr of propylene at a catalyst temperature of 650 K, and the results are displayed in Figure 1 in histogram form. Metallic molybdenum is inactive under these reaction conditions, and both MoO<sub>2</sub> and MoO<sub>3</sub> films catalyze olefin metathesis. Shown for comparison is the activity of a supported molybdenum oxide catalysts with a relatively high catalyst loading (18.6%),<sup>42</sup> where the agreement between the activities of the model catalysts and the high-surface-area sample is good. The temperature dependence of the metathesis rate is shown plotted in Arrhenius form (ln(rate) versus 1/T) in Figure 2. These results indicate that there are two distinct metathesis pathways. One predominates below  $\sim 650$  K, where the reaction activation energy is  $\sim 6$  kcal/mol (a value similar to that found for heterogeneous metathesis catalysts<sup>4,5</sup>) and where the absolute rate is similar to that for high-surface-area metathesis catalysts (Figure 1). Above 650 K, the reaction is dominated by a high-activation-energy ( $E_{\text{act}} \sim 60$  kcal/mol) pathway. It is proposed that both of these pathways operate simultaneously but that the vast differences in their activation energies (and also correspondingly in their pre-exponential factors) mean that each predominates in

(29) Bartlett, B.; Tysoe, W. T. *Catal. Lett.* **1977**, *44*, 37.

(30) Burwell, R. L.; Brenner, A. J. *J. Mol. Catal.* **1975**, *1*, 77.

(31) Thomas, R.; Moulijn, J. A. *J. Mol. Catal.* **1982**, *15*, 157.

(32) Wang, L. P.; Tysoe, W. T. *Surf. Sci.* **1990**, *230*, 74.

(33) Wu, G.; Bartlett, B.; Tysoe, W. T. *Surf. Sci.* **1997**, *373*, 129.

(34) Wang, L.; Soto, C.; Tysoe, W. T. *J. Catal.* **1993**, *143*, 92.

(35) Wu, G.; Bartlett, B.; Tysoe, W. T. *Surf. Sci.* **1997**, *383*, 57.

(36) Kennett, H. M.; Lee, A. E. *Surf. Sci.* **1975**, *48*, 606.

(37) Ko, E. I.; Madix, K. J. *Surf. Sci.* **1981**, *109*, 221.

(38) Bauer, E.; Hoppa, H. *Surf. Sci.* **1979**, *88*, 31.

(39) Zhang, C.; Van Hove, M. A.; Somorjai, G. A. *Surf. Sci.* **1985**, *149*, 326.

(40) Kennett, H. M.; Lee, A. E. *Surf. Sci.* **1975**, *48*, 624.

(41) Bartlett, B.; Schneerson, V. L.; Tysoe, W. T. *Catal. Lett.* **1995**, *3*, 1.

(42) Thomas, R.; Moulijn, J. A. *J. Mol. Catal.* **1982**, *15*, 157.

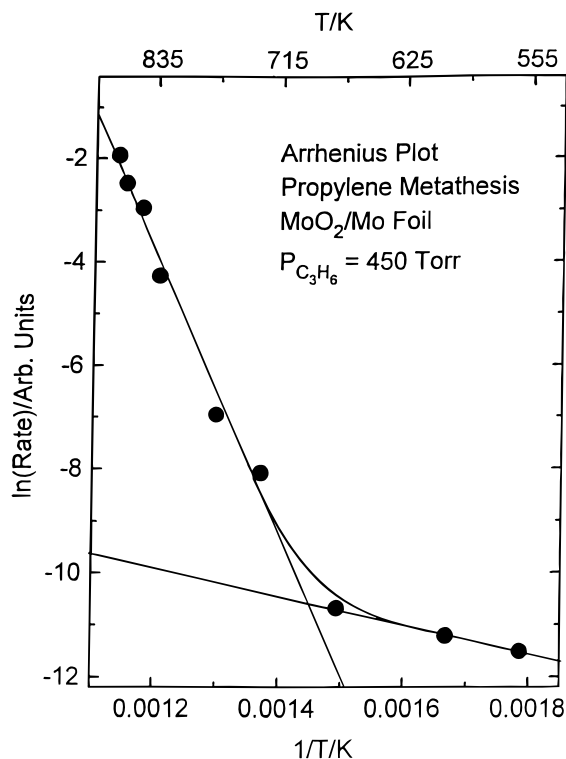


**Figure 2.** Arrhenius plot for propylene metathesis catalyzed by MoO<sub>2</sub> using 540 Torr of propylene, showing the two distinct reaction regimes.

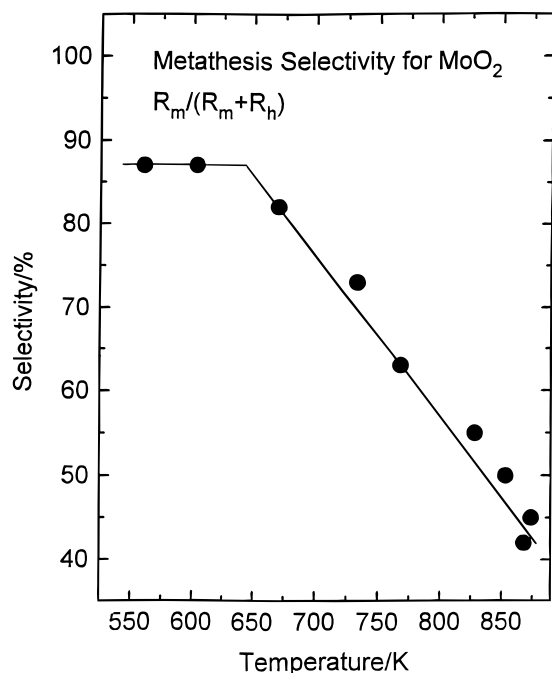


**Figure 3.** Selectivity for olefin metathesis catalyzed by MoO<sub>2</sub> plotted as a function of temperature using 450 Torr of propylene again showing two different reaction regimes.

a different temperature regime. Further evidence for different reaction pathways above and below 650 K comes from the plot of metathesis selectivity as a function of reaction temperature displayed in Figure 3. Here the selectivity is defined as the amount of ethylene and butene formed compared to the total of all hydrocarbons. In this case, the selectivity is rather high and constant below 650 K but decreases linearly with increasing reaction temperature above that temperature.

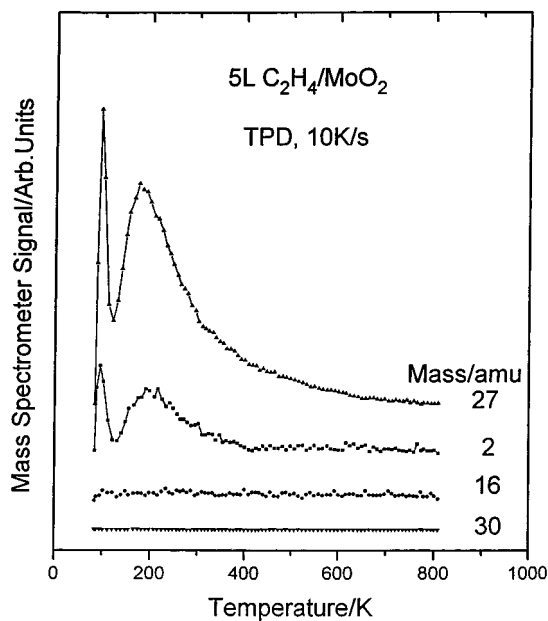


**Figure 4.** Temperature-programmed desorption spectra collected following exposure of MoO<sub>2</sub> to 5 L of ethylene, detecting 2, 16, 27, and 30 amu.

An MoO<sub>2</sub> film grown onto a polycrystalline molybdenum substrate appears to provide a reasonable model for a supported catalyst, and therefore its surface chemistry is investigated in ultrahigh vacuum. Shown in Figure 4 are a series of temperature-programmed desorption data collected following ethylene adsorption (5 L) at 80 K on MoO<sub>2</sub>. These results indicate that ethylene adsorbs molecularly on MoO<sub>2</sub> and desorbs intact at ~190 K. The sharp peak at ~100 K is due to a small amount of multilayer adsorption. A simple Redhead analysis yields a desorption activation energy of 11.1 kcal/mol using the commonly adopted value of  $1 \times 10^{13} \text{ s}^{-1}$  for the pre-exponential factor and using the experimental heating rate of 10 K/s. Similar results are obtained for other alkenes, for example, propylene<sup>43</sup> and butene,<sup>44</sup> adsorbed on MoO<sub>2</sub>, indicating that this is an extremely unreactive surface in ultrahigh vacuum, despite being an active catalyst under higher pressure conditions.

Fortunately, however, oxygen adsorbed on Mo(100) affects its catalytic activity. This is illustrated by the data in Figure 5, which displays the relative metathesis activity in the high-temperature (and high-activation-energy) regime, using 450 Torr of propylene at 870 K. Under these circumstances, metathesis is catalyzed by metallic molybdenum. The reactivity is, however, enhanced by the addition of oxygen to the surface, where the addition of about 0.5 monolayers leads to a substantial rate increase and coverages above a monolayer effectively poison the reaction. The chemistry of alkenes is followed, therefore, on molybdenum modified by various overlayers of oxygen. As noted above, these can be prepared relatively easily,<sup>36–39</sup> and also, as will be demonstrated below, they exhibit a rich variety of chemistry for various oxygen coverages.

It has been demonstrated that the binding energies of the 2s-derived molecular orbitals of a range of hydrocarbons can be calculated rather accurately using the Hückel theory,<sup>45,46</sup> that is, by taking the overlap integral  $S$  to be

(43) Wu, G.; Tysøe, W. T. *Surf. Sci.* **1997**, *391*, 134.

(44) Wu, G.; Tysøe, W. T. *Surf. Sci.*, in press.

(45) Potts, A. W.; Streets, D. G. *J. Chem. Soc., Faraday Trans. 2* **1974**, *70*, 875.

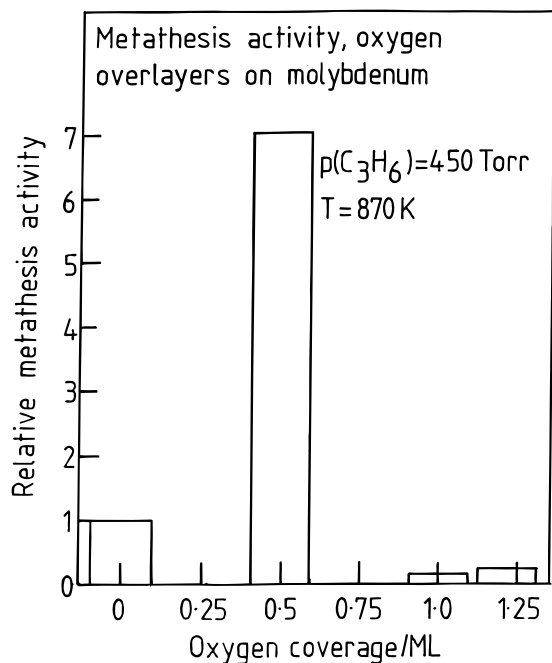


**Figure 5.** Relative propylene metathesis activity of various oxygen overlayers on molybdenum at a catalyst temperature of 870 K (in the high-temperature regime) using 450 Torr of propylene.

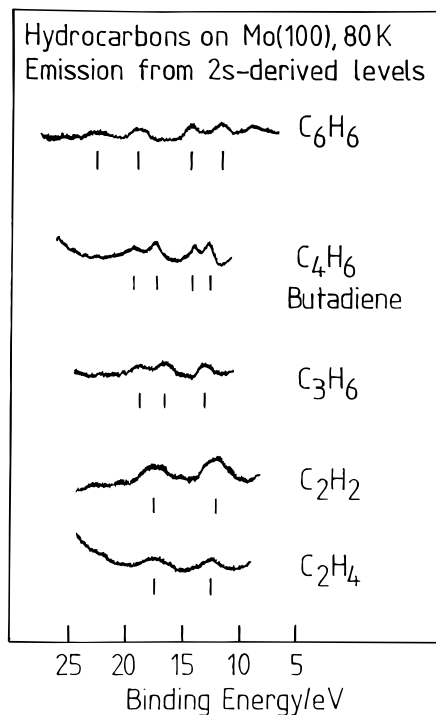


**Figure 6.** Ultraviolet photoelectron spectra of various hydrocarbons adsorbed on Mo(100) at low temperature ( $\sim 80$  K) collected using 60 eV photons, showing the 2s-derived molecular orbital region of the spectrum.

zero. This effect is illustrated in Figure 6, which displays the photoelectron spectra due to the emission from 2s-derived molecular orbitals of several hydrocarbons on molybdenum.<sup>47</sup> Note that these electrons have relatively large binding energies (between 10 and 25 eV) and so

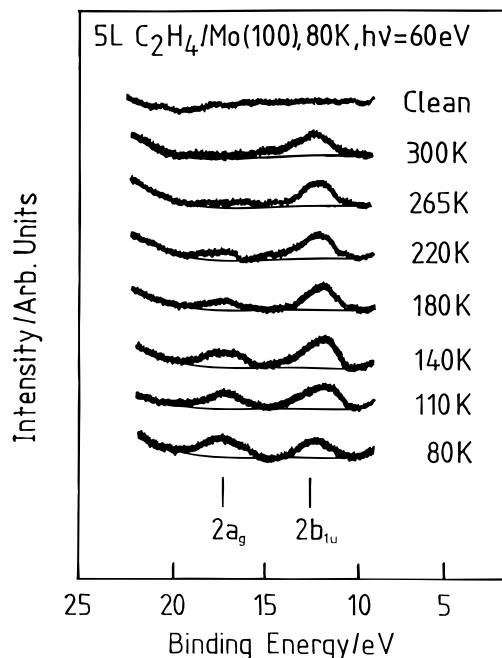


**Figure 7.** Ultraviolet photoelectron spectra obtained following exposure of Mo(100) to 5 L of ethylene at 80 K and after heating to various temperatures. Spectra were collected using 60 eV photons and display only the 2s-derived region of the spectrum.

qualify as shallow core levels. The peak positions are exactly what would be expected on the basis of simple molecular orbital calculations. This shallow core level spectroscopy is therefore sensitive to chemical changes at the surface, for example, bond scission reactions and so forth. This effect is illustrated by the spectra of Figure 7, which show the corresponding 2s region for ethylene adsorbed on metallic molybdenum at 80 K and heated to various temperatures. Two peaks are evident following adsorption at 80 K, which indicate that ethylene adsorbs molecularly at this temperature, and the peaks are assigned to  $2a_g$  and  $2b_{1u}$  bonding and antibonding features, respectively, as indicated on the figure. On heating, the higher binding energy feature decreases in intensity, so that by  $\sim 265$  K the spectrum consists of a single peak at a  $\sim 12.5$  eV binding energy, suggesting the formation of a surface  $C_1$  species. These results imply that molybdenum is capable of cleaving carbon-carbon double bonds in a relatively facile fashion. This chemistry is in complete contrast to that found on the group VIII metals where carbon-carbon bonds remain intact up to relatively high temperatures.

Further evidence for carbon-carbon bond cleavage for adsorbed ethylene is presented in Figure 8, which shows the 16-amu (methane) desorption spectra collected following adsorption of ethylene on oxygen-modified Mo(100) at 80 K. Methane is detected, although metallic molybdenum, despite photoelectron spectroscopic evidence that  $C_1$  species are formed (Figure 7), desorbs no methane. However, methane is detected from oxygen-covered surfaces where the maximum yield is found from a surface covered with 0.67 monolayers of oxygen. Methane is therefore proposed to form from carbene species produced by scission of the alkene double bond and subsequent hydrogenation of the methylene to methane. To test whether the latter step is feasible, methylene species were grafted on Mo(100) by adsorbing methylene iodide. The resulting temperature-programmed desorption spectrum is shown in Figure 9. A relatively small amount of methane is formed on Mo(100). However, pre dosing the

(46) Streets, D. G.; Potts, A. W. *J. Chem. Soc., Faraday Trans. 2* **1974**, *70*, 1505.

(47) Wang, L. P.; Hinkelman, R.; Tysoe, W. T. *J. Electron Spectrosc. Relat. Phenom.* **1991**, *56*, 341.

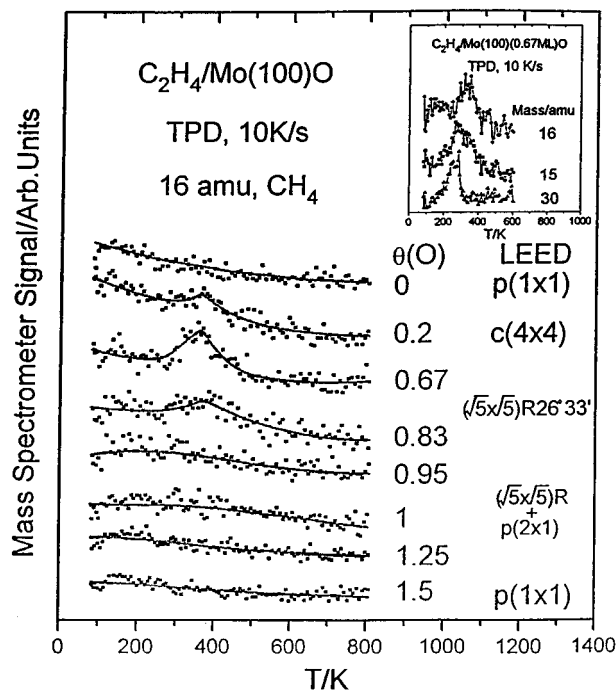


**Figure 8.** Temperature-programmed desorption spectra (16 amu,  $\text{CH}_4$ ) collected following adsorption of ethylene on various oxygen-covered Mo(100) surfaces. The oxygen coverages are displayed adjacent to the corresponding spectra. Shown as an inset are the 16, 15, and 30 amu spectra obtained following adsorption of ethylene on a Mo(100) surface covered by 0.67 monolayers of oxygen.

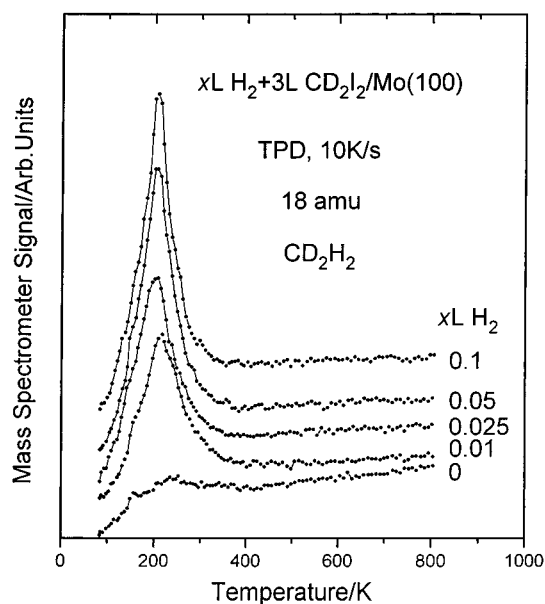


**Figure 9.** Thermal desorption spectra (18 amu,  $\text{CH}_2\text{D}_2$ ) collected by adsorbing methylene iodide on Mo(100) with various hydrogen precoverages. The hydrogen dose is displayed adjacent to each spectrum.

Mo(100) sample with only 0.01 L of hydrogen results in a substantial enhancement in the rate of methane formation. Higher hydrogen exposures lead to further, although less dramatic, increases in methane yield. Thus, adsorbed methylene species can react with surface hydrogen to form methane in accord with the above proposal.<sup>48</sup> Note that no ethylene was found to be formed either by coupling of methylene species on the surface after dosing

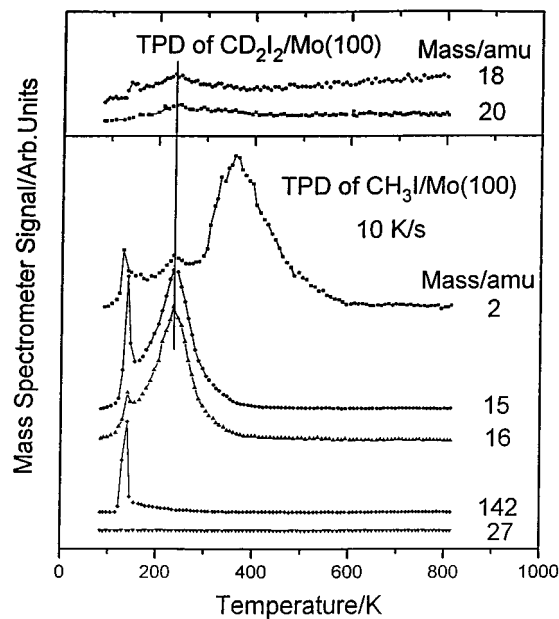


**Figure 10.** Hydrogen (2 amu), methane (15 and 16 amu), methyl iodide (142 amu), and ethylene (27 amu) temperature-programmed desorption spectra obtained following adsorption of methyl iodide on Mo(100). Shown for comparison is the methane thermal desorption spectra (18 and 20 amu) obtained by adsorbing  $\text{CD}_2\text{I}_2$  on Mo(100).

methylene iodide or by monitoring possible isotope-scrambling products after dosing the surface with  $^{13}\text{C}^{12}\text{CH}_4$ .

Insights into the reaction pathway to methane formation can be found from the data displayed in Figure 10, which shows a series of temperature-programmed desorption spectra collected by adsorbing methyl iodide onto Mo(100). Note that this surface has not been precovered with hydrogen, in this case, although significant yields of methane are found. Again, methane desorbs at  $\sim 230$  K. Shown as an inset are the corresponding desorption data for methylene iodide adsorbed on Mo(100) (see above). The methane desorption peak temperatures are identical although the yield is much lower in the latter case. This indicates that the rate-limiting step to methane formation is the addition of hydrogen to the methyl group to form methane rather than the initial addition of hydrogen to a carbene to form a methyl group.

The chemistry of other unsaturated hydrocarbons was examined on various oxygen-precovered surfaces in order to investigate whether similar reactivity patterns are found in these cases. Figure 11 shows the 29 amu (propane) desorption spectra obtained by adsorbing propylene onto a hydrogen-precovered Mo(100) surface as a function of hydrogen exposure. Clearly, molybdenum-catalyzed alkene hydrogenation and the catalytic reaction have been investigated at higher pressures.<sup>49</sup> The clear decrease in peak temperature as the hydrogen coverage increases indicates a second-order reaction with surface hydrogen. Note again the large increase in hydrogenation product yield with the addition of relatively small amounts of hydrogen. Methane is also synthesized with a desorption peak temperature and a variation in yield with oxygen coverage essentially identical with those found following ethylene adsorption (Figure 8), but the total yield is larger and methane desorption is also found from Mo(100).<sup>43</sup> In addition, no ethylene or ethane desorption was detected following the adsorption of propylene on any oxygen-covered Mo(100) surfaces.

(48) Weldon, M. K.; Friend, C. M. *Surf. Sci.* **1994**, *321*, L202.

(49) Wang, L.; Tysoe, W. T. *Catal. J.* **1991**, *128*, 320.

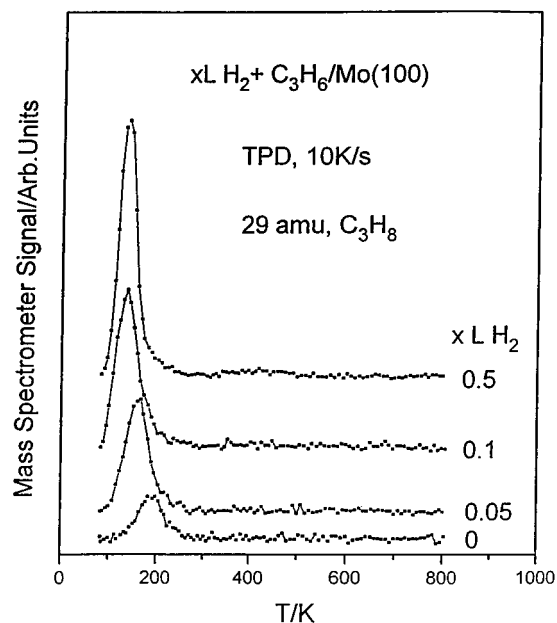


**Figure 11.** Temperature-programmed desorption spectra (29 amu, propane) obtained by adsorbing propylene on a hydrogen precovered surface as a function of hydrogen exposure. Hydrogen exposures are marked adjacent to each spectrum.

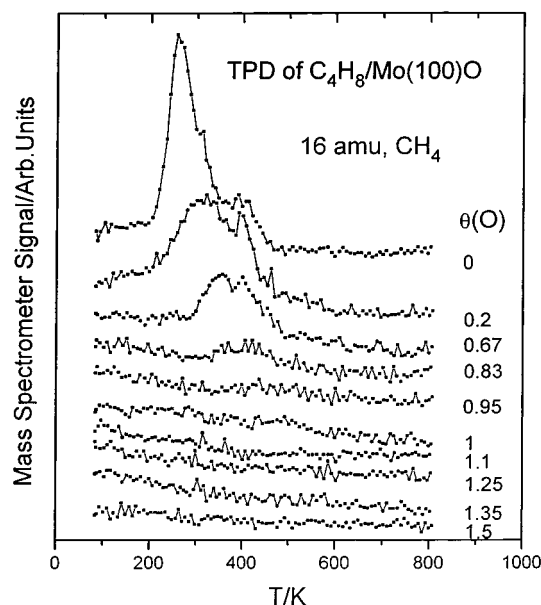


**Figure 12.** Temperature-programmed desorption spectra (16 amu, methane) collected after exposing various oxygen precovered surfaces to 2-butene. The oxygen coverages are marked adjacent to each spectrum.

The corresponding methane desorption data obtained following 2-butene adsorption on Mo(100) are displayed in Figure 12, where again substantial amounts of methane are formed. Now the peak temperature varies with oxygen coverage, so that on metallic molybdenum, methane desorbs at  $\sim 260$  K, close to the temperature found for methane desorption after dosing either methylene iodide or methyl iodide on these surfaces. There is also a small feature evident at 400 K after 2-butene adsorption on Mo(100). The low-temperature feature shifts to higher temperatures with increasing oxygen coverage, and the 400 K peak position remains essentially unaffected. The yield decreases with increasing oxygen coverage although the amount of methane formed is considerably larger than that for both ethylene and propylene adsorption. The only

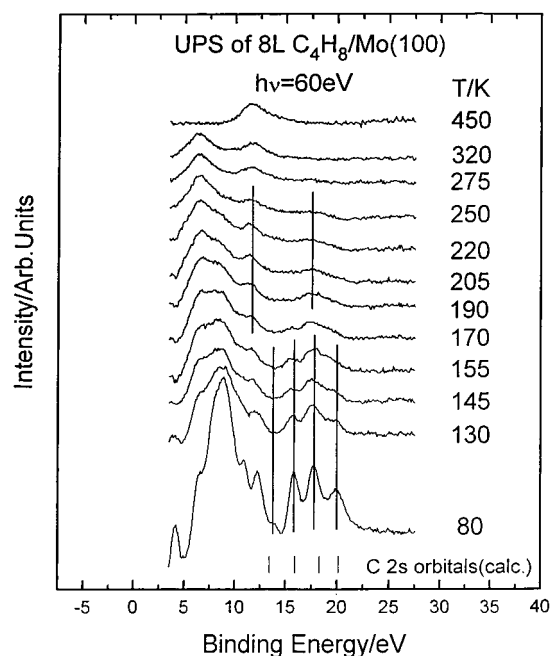


**Figure 13.** Ultraviolet photoelectron spectra collected using 60 eV photons following adsorption of 2-butene on Mo(100) as a function of annealing temperature. Annealing temperatures are marked adjacent to each spectrum. Also indicated are the positions of peaks calculated for the 2s-derived molecular orbitals of 2-butene and the corresponding positions for a  $C_2$  hydrocarbon.

other reaction pathways noted for 2-butene adsorption on Mo(100) and oxygen-modified Mo(100) were hydrogenation to butene and complete dehydrogenation to carbon and hydrogen. No other  $C_3$  or  $C_2$  hydrocarbons were detected.

To probe possible reaction pathways for 2-butene on Mo(100), photoelectron spectra were collected using 60 eV photons as a function of annealing temperature. The results are displayed in Figure 13. The traces are obtained by subtracting the spectrum of clean Mo(100) from those of adsorbate-covered surfaces in order to emphasize the adsorbate-induced features. Particularly emphasized are the 2s-derived orbitals. The experimental positions for a condensed 2-butene layer (formed at 80 K) are compared with binding energies calculated for 2-butene using the prescription outlined by Potts.<sup>45,46</sup> The agreement between these values is good, further confirming the efficacy of the method. The multilayer desorbs on heating the sample to  $\sim 130$  K, resulting in a significant attenuation in intensity. Nevertheless, the positions of the peaks, in particular those in the 2s region, are identical with those for the molecular overlayer, indicating that 2-butene adsorbs molecularly at this temperature, in accord with the temperature-programmed desorption results that hydrogenation products are formed. The peak positions remain essentially unchanged up to  $\sim 155$  K. Two peaks are formed on heating to  $\sim 190$  K, indicating the formation of a  $C_2$  hydrocarbon. Further heating to 275 K reveals the presence of only a single peak at a binding energy of 12.5 eV consistent with the detection of methane in temperature-programmed desorption (Figure 12). It is important to note that there is no evidence for the intervention of any other  $C_4$  or  $C_3$  species that precedes the formation of an adsorbed  $C_2$  hydrocarbon. This implies that the carbon-carbon double bond cleaves via a reaction analogous to that seen above for ethylene, which, in the case of 2-butene, leads to the formation of methylcarbenes (the  $C_2$  hydrocarbon detected between 190 and 250 K).

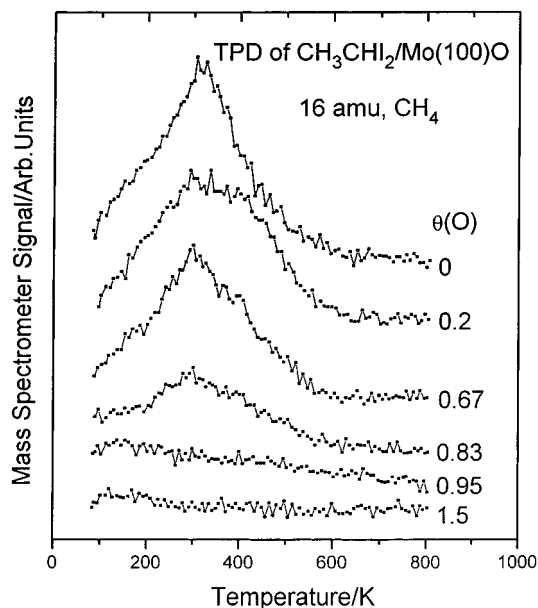


**Figure 14.** Temperature-programmed desorption spectra collected (16 amu, methane) after exposing various oxygen precovered surfaces to 1,1-diiodoethane. The oxygen coverages are marked adjacent to each spectrum.

To further examine the reactivity of methyl carbenes on oxygen-covered Mo(100), the surface was exposed to 1,1-diiodomethane, and the resulting methane desorption spectra obtained for various oxygen-covered surfaces are displayed in Figure 14. Clearly adsorbed ethylidene species can thermally decompose to form methane on both Mo(100) and oxygen-modified Mo(100). As noted above, no  $C_2$  hydrocarbons are detected following 2-butene adsorption on any molybdenum-derived surface. However, ethylene is detected after adsorbing 1,1-diiodoethane on oxygen-covered molybdenum.<sup>50</sup> Note that an exactly identical peak is noted following ethyl iodide adsorption, suggesting that ethylene forms by  $\beta$ -hydride elimination from an adsorbed ethyl species formed by partial hydrogenation of the  $\alpha$ -carbon of the carbene. Note, however, this reaction pathway is only seen for higher oxygen coverage ( $\theta_0 > 0.95$ ), whereas the data of Figure 13 suggest that methyl carbenes form for oxygen coverages less than 1.0, since methane desorption is only detected in this coverage range.

Finally, shown plotted in Figure 15 is the methane yield for ethylene (●), propylene (▲), and 2-butene (▼) adsorbed on various oxygen-covered surfaces. Note that the total methane yield increases with increasing carbon number. However, the methane yield from ethylene peaks at an oxygen coverage of  $\sim 0.6$  and is zero for  $\theta_0 = 0$  and 1.0. The methane yield from 2-butene decreases linearly with increasing oxygen coverage, and the yield from propylene is essentially a linear combination of the two effects.

### Discussion

Model olefin metathesis catalysts consisting of either  $MoO_2$  or  $MoO_3$  formed by oxidizing a molybdenum foil mimic the activity of supported metathesis catalysts for reaction below  $\sim 650$  K (Figure 1). This reaction is also catalyzed in the homogeneous phase and is suggested to be initiated by the formation of a carbene, which is then proposed to react to form a metallacycle that thermally decomposes by the reverse of this route to yield metathesis products.<sup>10–36</sup> Simultaneously, there is a high-

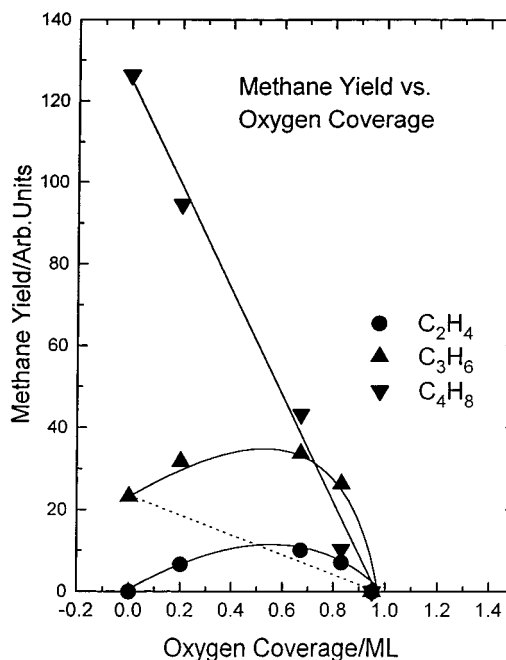


**Figure 15.** Plot of the methane yield versus oxygen coverage for ethylene (●), propylene (▲) and 2-butene (▼) on oxygen-covered Mo(100).

activation-energy reaction pathway that predominates at high temperatures and where the activation energy is much higher ( $\sim 60$  kcal/mol) (Figure 2). Unfortunately, these model oxide catalysts are rather inactive in ultrahigh vacuum so that alkenes merely adsorb and desorb molecularly and essentially undergo no surface chemistry (Figure 4). However, oxygen overlayers on Mo(100) do affect the metathesis activity of the catalyst in the higher temperature regime (Figure 5), so that the chemistry of alkenes is studied on this surface. This turns out to exhibit a rather rich surface chemistry which reveals significant variations in reactivity as a function of oxygen coverage. This is illustrated by the data of Figures 7 and 8, which show that ethylene adsorbs dissociatively on oxygen-covered molybdenum surfaces to yield surface carbenes. Grafting methylene and methyl species onto the surface by thermally decomposing iodine-containing precursors indicates that carbenes can react with adsorbed hydrogen to form methane and that the rate-limiting step for this reaction is the final addition of hydrogen to a methyl species, presumably indicating that the first step is fast. The activation energy for methane formation, in the absence of coadsorbed iodine, is measured from a leading-edge plot and yields an activation energy to methane formation of  $\sim 23$  kcal/mol. Previous estimates of the heat of adsorption of carbenes have yielded values  $\sim 100$  kcal/mol.<sup>33</sup> The data of Figure 10 indicate that hydrogenation of a methyl group is, in fact, rate limiting, which allows the heat of adsorption of a methyl group to be estimated from

$$E(CH_4) \sim \Delta H_{(ads)}(CH_3) + \Delta H_{(ads)}(H) - D(CH_3-H)$$

where  $\Delta H_{(ads)}(H)$  is the heat of adsorption of hydrogen on Mo(100) ( $\sim 60$  kcal/mol<sup>51</sup>) and  $D(CH_3-H)$  is the strength of the  $CH_3-H$  bond (104 kcal/mol<sup>52</sup>). Using the activation energy for the formation of methane measured above, this

(51) Han, H. R.; Schmidt, L. D. *J. Phys. Chem.* **1971**, *75*, 227.

(52) Weast, R. C., Ed. *Handbook of Chemistry and Physics*; Chemical Rubber, Co.: Cleveland, OH, 1967.

(50) Wu, G.; Tysoe, W. T. In preparation.

yields an approximate value for the heat of adsorption of a methyl group of  $\sim 69$  kcal/mol. Since the hydrogenation of this to methane is the rate-limiting step, the activation energy of hydrogenation of a methylene to a methyl group will be less than this value, so that  $\Delta H_{\text{(ads)}}(\text{CH}_2)$  is less than 128 kcal/mol but substantially greater than 69 kcal/mol. However, reacting ethylene over metallic molybdenum leads to a series of higher hydrocarbons with a distribution that is well described by a Schulz–Florey plot.<sup>29</sup> This suggests that the high-temperature metathesis reaction (Figures 2 and 3) is due to alkene dissociation and recombination of the resulting carbene species on the metal surface. The high activation energy for this reaction then reflects the large heat of adsorption of carbene species. The activation energy for this reaction at high temperature ( $\sim 60$  kcal/mol<sup>29</sup>) can be used to estimate a carbene heat of adsorption<sup>33</sup> and yields a value of  $\sim 120$  kcal/mol, in good agreement with the range estimated above. Note that this is an “active site” removal pathway for the carbene metathesis mechanism which may operate at lower temperatures.<sup>10–26</sup> The large activation energy for this pathway means that these species are removed only slowly at lower temperatures.

It is clear, at least on these oxygen-modified surfaces, that carbene formation is rather facile. We turn our attention now to examining the way in which these species form. Note that both propylene and 2-butene yield methane, indicating that they ultimately decompose to form either methyl or methylene species that subsequently hydrogenate to form methane. The other major reaction pathways are hydrogenation to form alkanes and complete thermal decomposition, forming carbon and hydrogen. No other products are formed. It has been suggested that carbenes can be formed from alkenes containing alkyl groups by alkyl dehydrogenation.<sup>53,54</sup> Under this proposal, the methyl group of propylene would react to form an allylic species. Hydrogenation of the allylic species at the  $\beta$  position would lead to the formation of a metallacycle which would then thermally decompose to yield ethylene and deposit a carbene. Note, first, that no ethylene is detected following propylene adsorption. Second, adsorbing  $\text{CH}_2=\text{CH}-\text{CH}_2\text{I}$  to form the allylic species onto various oxygen-modified surfaces results in the desorption of only hydrogen.<sup>55</sup> Predosing the surface with hydrogen to attempt to hydrogenate this species at the  $\beta$ -position merely yields a small amount of propane. An alternative pathway proposes partial hydrogenation of adsorbed alkenes to yield alkyl species.<sup>56</sup> This clearly takes place, since alkenes react to form alkanes, which must proceed via an intervening alkyl species. The alkyl species is then proposed to decompose via an  $\alpha$ -hydride elimination. In fact, alkyl species grafted onto these surfaces by adsorbing ethyl iodide thermally decompose to form ethylene via a  $\beta$ -hydride elimination, as generally found on transition metal surfaces.

As noted above, the ultraviolet photoelectron spectroscopic data of Figure 13 indicate that 2-butene thermally decomposes directly to form  $\text{C}_2$  species (proposed to be methyl carbenes) without the participation of any other surface  $\text{C}_4$  species. Both of the mechanisms outlined above would involve the intervening formation of other  $\text{C}_4$  species, the former pathway involving a methylmetallacycle and the latter involving a methylethylcarbene. The

formation of either of these intermediates would lead to significant changes in the 2s-derived peak positions, which are not detected.

Additional catalytic evidence for the formation of a combination of carbene and methylcarbene in the olefin metathesis pathway at high temperatures is that the distribution of higher hydrocarbon products can be calculated using a copolymerization model<sup>57</sup> analogous to the Schulz–Florey distribution<sup>29</sup> that accurately predicts the higher hydrocarbon distribution from ethylene. Note, however, that, for the proposed model to be correct, the methylcarbene should thermally decompose to form methane in ultrahigh vacuum, since this is the only hydrocarbon product found following the adsorption of either propylene or 2-butene. This can be probed by grafting methylcarbenes (ethylidenes) onto the surface by exposing it to 1,1-diiodoethane and monitoring the methane signal (Figure 14). Clearly, a large amount of methane is formed in the temperature range found following 2-butene and propylene adsorption. In addition, the methane yield is a maximum for clean Mo(100) and decreases linearly with increasing oxygen coverage. This distribution in methane yield is similar to that found following the adsorption of 2-butene. For oxygen coverages between  $\sim 1.0$  and 1.5, ethylene is formed from ethylidene. A similar ethylene desorption state is found after adsorbing ethyl iodide on oxygen-modified Mo(100), which is presumably formed via a  $\beta$ -hydride elimination pathway.<sup>50</sup> Thus, ethylene formation from ethylidene likely involves hydrogenation at the  $\alpha$ -carbon to form an ethyl species and a rate-limiting  $\beta$ -hydride elimination. Final evidence for direct carbon–carbon bond cleavage comes from the data of Figure 15, which plots the methane yield as a function of oxygen coverage. The yield of methane from 2-butene decreases linearly with oxygen coverage in the same way as found when exposing the surface to 1,1-diiodoethane. In contrast, the methane yield from ethylene, which is proposed to react to form adsorbed  $\text{CH}_2$  species, is zero both for clean Mo(100) and when the oxygen coverage is unity and reaches a maximum at some intermediate coverage ( $\theta_{\text{O}} \sim 0.67$ ). The distribution of the yield of methane from propylene on various oxygen-covered surfaces is a combination of these two trends, as would be expected, since propylene forms both carbenes and methylcarbenes.

Evidently the total methane yield increases substantially in going from ethylene to propylene to 2-butene. Since it is proposed above that methane forms via a carbon–carbon double-bond dissociation reaction to form carbenes, the variation in methane yield may be related to this dissociation probability. It has been suggested that, within the context of the Dewar–Chatt–Duncanson model, alkenes bond on Mo(100) primarily by donation of electrons from  $\pi$ -orbitals to the metal rather than via back-donation into vacant  $\pi^*$  orbitals.<sup>58,59</sup> That is, alkenes behave like  $\pi$ -donors on Mo(100). Corroborative evidence for this idea comes from the effect on the energetics of alkene desorption,<sup>35,43</sup> where the desorption activation energies increase with the addition of oxygen to the surface in accord with the above proposal. It should be emphasized that alkenes are likely to bond synergistically via both donation and acceptance of electrons but that electron donation to the surface predominates. The relatively large

(53) Ephritikhine, M.; Green, M. L. H. *J. Chem. Soc., Chem. Commun.* **1976**, 926.

(54) Adams, G. J. A.; Davis, S. G.; Ford, K. A.; Ephritikhine, M.; Todd, P. F.; Green, M. L. H. *J. Mol. Catal.* **1980**, *8*, 15.

(55) Wu, G.; Tysoe, W. T. In preparation.

(56) Laverty, D. T.; Rooney, J. J.; Stewart, A. *J. Catal.* **1976**, *45*, 110.

(57) Bartlett, B. F. Ph.D. Thesis, University of Wisconsin–Milwaukee, 1997.

(58) Deffeyes, J. E.; Smith, A. H.; Stair, P. C. *Appl. Surf. Sci.* **1986**, *26*, 517.

(59) Deffeyes, J. E.; Smith, A. H.; Stair, P. C. *Surf. Sci.* **1985**, *163*, 79.



number of vacant d-orbitals in molybdenum in comparison with, for example, group VIII metals may partially rationalize the bonding mode in this case. The position of the  $\pi$ -orbital in alkenes is substantially affected by the presence of a methyl group, so that the binding energy of the  $\pi$ -orbitals is 10.5 eV in ethylene 9.7 eV in propylene, and 9.1 eV in 2-butene.<sup>61</sup> These shifts are fairly substantial and indicate that the  $\pi$ -orbital should be rather closer to the Fermi level in 2-butene than in ethylene. This indicates that the extent of electron donation from the  $\pi$ -orbitals to the substrate should be larger for 2-butene than for ethylene leading to a larger decrease in bond order and therefore an increased bond dissociation probability in the order 2-butene > propylene > ethylene, as found experimentally.

### Conclusion

Alkenes react on oxygen-covered Mo(100) to form alkanes, completely thermally decompose to form carbon and hydrogen, or dissociatively decompose to form carbene

---

(60) Robinson, J. W., Ed. *Handbook of Spectroscopy*; Chemical Rubber, Co.: Cleveland, OH, 1974; Vol. I.

species. Both model molybdenum oxides and oxygen-covered Mo(100) catalyze olefin metathesis, where two reaction pathways are found: one that predominates at low temperature (<650 K) and has a relatively low activation energy and another that predominates at higher temperatures and has a much higher activation energy of ~60 kcal/mol. This reaction is proposed to proceed by recombination of the carbene fragments which adsorb relatively strongly to Mo(100) with a heat of adsorption of ~120 kcal/mol, which accounts for the rather high activation energy for this reaction, and which are formed relatively rapidly on oxygen-covered Mo(100) surfaces.

**Acknowledgment.** We gratefully acknowledge support of this work by the U.S. Department of Energy, Division of Chemical Sciences, Office of Basic Energy Sciences, under Grant No. DE-FG02-92ER14289. This work is based upon research conducted at the Synchrotron Radiation Center, University of Wisconsin—Madison, which is supported by the NSF under Award No. DMR-95-31009.

LA970735Q